SEVENTH EUROPEAN ROTORCRAFT AND POWERED LIFT AIRCRAFT FORUM

Paper No 47

SOME UNSTEADY AERODYNAMIC EFFECTS ON HELICOPTER ROTORS

P G Wilby
M J Riley
Judith Miller

Royal Aircraft Establishment

Farnborough, UK

September 8 - 11, 1981

Garmisch-Partenkirchen
Federal Republic of Germany

Deutsche Gesellschaft für Luft- und Raumfahrt e. V.

Goethestr. 10, D-5000 Köln 51, F.R.G.

SOME UNSTEADY AERODYNAMIC EFFECTS ON HELICOPTER ROTORS

P G Wilby, M J Riley, Judith Miller

Royal Aircraft Establishment, UK

1 INTRODUCTION

It is well known that unsteady effects have an important influence on the aerodynamic loading experienced by a helicopter rotor in forward flight. These effects include dynamic stall characteristics with the associated stall delay and large nose-down change in pitching-moment. All unsteady effects must be taken into account when predicting rotor loads, performance and flight envelope, thus it is important that all these effects be fully appreciated and understood. However, one must remember that the full unsteady effects on the rotor result from simultaneous oscillatory variations of both incidence and Mach number, and it is difficult to study these effects in isolation from the rest of the rotor environment. For example, the effects of oscillatory pitch are usually studied experimentally at a steady free-stream Mach number. Empirical methods for modelling these effects, especially dynamic stall characteristics, are developed on the basis of such experiments and then incorporated in the rotor loads prediction methods. One of the questions we need to answer is whether or not this approach neglects any important effects. This paper presents some results from a programme of work involving oscillatory aerofoil tests, flight experiments and unsteady aerodynamic prediction methods in an attempt to answer this question.

2 RETREATING BLADE STALL

Over the past 10 to 15 years most helicopter manufacturers and research establishments have been developing new rotor blade sections, and one of the main design aims has been to delay the onset of retreating blade stall. This can be achieved through increasing the value of $C_{l_{max}}$ at the low values of Mach number (typically around 0.3) found near the tip of the retreating blade in cruise conditions. The development of such aerofoils requires wind tunnel tests in two-dimensional conditions, and these have usually been carried out at steady values of incidence. However, the need for tests involving oscillatory pitching motion so as to understand dynamic stall characteristics has long been recognized, and the author has previously pointed out[1] that oscillatory tests may be required in order to assess the true two-dimensional steady stall incidence. Even after carrying out oscillatory pitch tests it is still not certain that the results will be the same as those obtained on a rotor in forward flight, where the free stream Mach number varies, the environment is perhaps more three-dimensional and there are no wind-tunnel interference effects.

An example of the sort of questions that are still left unanswered by oscillatory two-dimensional tests is provided by results for one of the recent RAE aerofoils, the RAE 9647 profile. First of all this aerofoil was tested in steady conditions, and the measured variation of normal force coefficient C_N with incidence is shown in Fig 1 for a free-stream Mach number M_∞ of 0.3. The stall incidence is seen to be 14.5°. The aerofoil was then tested with an oscillatory pitching motion, and the other results shown in Fig 1 are for a very low reduced frequency ($\nu = 0.008$) - referred to as quasi-steady conditions - where no significant unsteady effects would be expected. However, stall did not occur in these tests until an incidence of 18° was reached. With the model pitching at a reduced frequency that represents the once per resolution frequency of a full scale rotor, the results shown in Fig 2 were obtained. These results were obtained with fixed frequency and amplitude, but with

the mean incidence being progressively increased. Here, stall occurs once the maximum incidence exceeds 17.5°. In Ref 1 it was argued that this is the true steady stall incidence and that significant dynamic stall delay only occurs if incidence continues to increase beyond this value at a sufficiently high pitch rate. A possible explanation for the low values of stall incidence measured in steady conditions is suggested by the test techniques used. All these tests were carried out at the Aircraft Research Association (ARA) at Bedford and the wind-tunnel used is of the intermittent type. For steady tests, incidence remains fixed throughout each run, and at high angles of incidence it may be that the flow over the model is separated during the initiation of the tunnel flow. When full tunnel air speed is obtained, the flow over the model remains separated or re-attaches, depending on the value of incidence. If this is the case, then the test conditions correspond to those in which tunnel speed is held constant while incidence is slowly decreased from stalled conditions to unstalled conditions. Results for C_N plotted against α would then tend to fall on the lower part of the well known steady stall hysteresis loop. The upward stroke at very low frequency would of course produce results on the upper branch of the steady stall hysteresis loop, with a higher value of stall incidence. Even though a plausible explanation can be offered for the differences, found in Fig 1, there is still the knowledge that the presence of the tunnel walls has an influence on stall incidence, and this leaves a certain amount of uncertainty as to the value of stall incidence that would be found on the full scale rotor. To this, we can add the uncertainty over the influence of the variations in free-stream Mach number that occur on the rotor. In order to try to remove these uncertainties, a flight experiment was devised at the RAE (Bedford) using a Puma helicopter.

Part of one of the main rotor blades was modified so that a balsa wood and glass-fibre fairing could be built around the blade to give the RAE 9647 profile. The resulting configuration is shown in planview in Fig 3. The RAE 9647 profile extends across two blade pockets, with a blending region of one pocket length at each end, over which the profile returns to that of the basic blade. At the centre of the modified region (81.6% rotor radius), a chordwise array of pressure sensors was installed at the positions given in Table 1. Further sensors were placed at several radial positions, as shown in Fig 3, all of them being at 2% chord. The latter were to be used to give an indication of leading-edge suction peak height and hence the spanwise incidence distribution. As a major objective of the experiment was to study dynamic stall characteristics in flight, it was important to ensure that the modified portion of the blade could be forced into stall within the safe flight envelope of the helicopter. The modification to the blade was therefore designed to set the RAE 9647 profile at 1.5° incidence relative to the basic blade. Wind-tunnel tests had shown that the RAE 9647 stall incidence at $M = 0.3$ is 2.5° higher than for NACA 0012 which is similar to the Puma blade section. Thus ideally the RAE 9647 profile should have been set at 2.5° incidence relative to the basic blade. However, it was felt that this might result in too great a penetration into supercritical conditions on the advancing side of the disc, with the danger of shock induced separation and the generation of a strong pitch disturbance.

In comparing flight and wind-tunnel measurements of chordwise pressure distributions there is one fundamental difficulty which is the absence of any true measure of blade incidence in flight. One must therefore seek comparisons that do not require a knowledge of incidence, and this led us to look for the maximum value of normal force coefficient C_N that could be achieved without incurring dynamic stall. So as to provide the best possible comparison with the tunnel tests it was necessary to ensure that the Mach number of the flight test section, at the point when maximum C_N was obtained, was as near as possible to the wind-tunnel test value of 0.3. It was also necessary to be able to determine whether or not stall occurred. Initially it was thought that a sudden and large drop in leading-edge suction peak would be an

Upper Surface	Lower Surface
0	0.01
0.005	0.04
0.01	0.10
0.02	0.22
0.03	0.46
0.05	0.68
0.075	0.90
0.1	
0.125	
0.15	
0.2	
0.3	
0.5	
0.7	
0.9	
1.0	

TABLE 1 - CHORDWISE POSITIONS OF PRESSURE SENSORS

adequate indication of retreating blade stall, but it will be seen that this is not a fool-proof criterion. A more reliable method is to plot the variation of pressure close to the leading-edge against C_N, as is done for the tunnel tests in Fig 4. Results for three test cases are shown in which frequency and amplitude are kept constant, but mean incidence progressively increased. Fig 4 also shows the variation of pitching-moment coefficient C_m with C_N, as the large nose-down change in C_m is the important feature of dynamic stall. For the lowest value of mean incidence it is seen that on the downstroke the suction peak and the value of C_m are both higher, for a given value of C_N, than on the upstroke. This is to be expected for attached flow. With the highest mean incidence both the suction peak and C_m take a sudden downwards plunge at the maximum value of C_N. For the intermediate value of mean incidence, the plunge in suction peak and C_m comes after C_N has fallen some way below its maximum value. However, both the last two cases show features that one expects to see during dynamic stall in which leading-edge separation occurs, giving a collapse in the leading-edge suction peak. As the resulting vortex travels towards the trailing-edge, generating a local increase in lift, a strong nose-down pitching moment is developed. One can deduce from Fig 4 that at the particular frequency chosen, stall does not occur during the first cycle for which a maximum value of 1.73 is reached, but it does occur in the second cycle when a $C_{N_{max}}$ of 1.8 is attained. Thus the maximum possible value of C_N that can be reached without stall lies somewhere between these two. It should be noted that the reduced frequency for these tests corresponds very closely to that for the Puma blade at once per revolution, and the amplitude of the incidence variation was $\pm 5^{\circ}$.

Let us now turn to the flight results and look for test conditions that correspond to those appropriate to Fig 4. In Fig 5 we have the variation of C_N with azimuth angle ψ as measured on the RAE 9647 profile in flight over a range of values of advance ratio μ. The outstanding feature of these plots is the sudden drop in C_N on the retreating side of the disc that occurs even at the lowest value of μ. This is accompanied by a sudden drop in leading-edge suction peak, which on its own might have suggested blade stall. When the variation of pressure coefficient at 0.5% chord, and C_m, with C_N is examined in Fig 6 however, there is no really clear

evidence of stall until the highest value of μ is reached. The blade section is definitely clear of stall at $\mu = 0.28$, and at $\mu = 0.335$ there is no collapse of leading-edge suction but there is an appreciable nose-down change in C_m. This is presumably the beginning of stall, and the maximum value of C_N is 1.76 which falls in the narrow band for maximum unstalled value deduced from wind-tunnel tests. The blade Mach number at the moment when $C_{N_{max}}$ was reached was 0.303 which is exactly the value for the wind-tunnel tests. Thus, these flight results suggest that the oscillatory aerofoil tests have in fact given a very good representation of dynamic stall onset as found on a rotor in flight.

Having decided that the sudden drop in C_N at low μ is not due to stall, we must find some other explanation. This is provided in Fig 7 which shows the intersection of the blade measuring station, at 81% rotor radius, with the tip locus of the preceding blade. For $\mu = 0.22$ this intersection takes place at an azimuth angle of 250° which is where the sudden drop in C_N begins. This sudden change in C_N must be due to the rapid and large change of incidence that occurs as the blade passes over the vortex generated by the preceding blade tip. It is seen in Fig 5 that the position of the C_N trough moves to a higher value of azimuth as μ increases, as does the vortex crossing. However, we note that the azimuthal position of the peak value of C_N does not vary with advance ratio, staying fixed at about $\psi = 250^\circ$, and further possible influences on blade incidence were looked for. By looking at the azimuthal variation of pitch link load, as shown in Fig 8 we see that an oscillatory torsional moment is building up as advance ratio increases above 0.22. This will produce a torsional motion that will contribute to the blade incidence. As the frequency is quite high - approximately 6 per revolution - there are also likely to be appreciable unsteady effects. It is seen that a trough in pitch link load occurs at $\psi = 250^\circ$ and such a trough corresponds to an incidence peak in the associated torsional motion. This local increase to blade incidence will contribute to the C_N peak that is found at $\psi = 250^\circ$. The cause of the torsional motion has not been fully explored but it is suspected that blade stall, inboard of the test section, is the cause. At the high value of thrust coefficient at which the measurements were made, it is likely that stall will occur near the front of the rotor disc due to the influence of the preceding blade tip vortex. This has been noted in earlier flight experiments on the Puma at the RAE. Evidence of the influence of blade stall on the torsional motion and blade incidence is seen in Figs 5, 6 and 8 for $\mu = 0.367$. Fig 6 tells us that the test section penetrates well into stall at this value of μ ; Fig 8 shows that this results in an extra peak in pitch link load in the fourth quadrant, and Fig 5 shows a large extra peak in C_N and hence incidence.

The fact that the rest of the blade stalls before the test section does is shown in Fig 9 where the spanwise variation of pressure coefficient at 2% chord is presented for three values of azimuth. At $\psi = 210^\circ$ there is a reasonably smooth variation with suction peak decreasing towards the blade tip. When the blade has moved to 235° azimuth the magnitude of the leading-edge suction peak has grown considerably for the RAE 9647 section but has changed very little on the basic blade. At 245° azimuth the RAE 9647 suction peak, and hence incidence, has grown still further, but there has been a definite collapse of suction peaks on the remainder of the blade. There is no possible reason for a large and abrupt change in incidence along the span, and the only explanation for these results is stalling of the basic blade. This is further confirmation of the wind tunnel tests which showed that the RAE 9645 section stalls at a higher incidence than NACA 0012, which is similar to the basic blade section of the Puma. The tunnel tests gave a difference of 2.5° in stall incidence at M = 0.3. For the flight tests, the RAE 9647 section was set at 1.5° higher incidence than the basic blade and was still unstalled well after the basic blade had stalled.

With separated flow on either side of the test section there is the possibility of contamination of the flow over the test section, and clearly factors are introduced that complicate the interpretation of measurements. In an attempt to reduce these influences, a further series of tests is being carried out with some leading-edge droop added to the basic blade in the vicinity of the test section. This droop should delay stall over this part of the blade.

3 FORE AND AFT SECTORS OF THE ROTOR

The next area of interest with regard to unsteady effects is the outer part of the blade as it passes through the fore and aft sectors of the disc. Here the value of:

$$\frac{d\alpha}{dt}$$

would be at its highest for a purely 1st harmonic variation, and also:

$$\frac{dM}{dt}$$

is at its highest value. The question that needs to be answered is whether or not the variation of M has a significant influence on the pitch rate effects. In attempting to answer this question we seek to compare flight measurements of pressure distributions with those obtained in oscillatory aerofoil tests. The difficulty once again is the absence of any precise measure of blade incidence in flight.

In comparing flight and oscillatory aerofoil measurements it is natural to choose a flight case where unsteady effects are large, ie where:

$$\frac{d\alpha}{dt}$$

is as large as possible. As the incidence variation between advancing and retreating sides of the disc increases with advance ratio, one is automatically led towards the high μ cases. Also it was felt that the most interesting case was likely to be one with supercritical flow which would only occur at the higher values of incidence encountered at high thrust coefficients. However, at high μ and C_T we have seen that a pronounced torsional oscillation of the blade was excited, and this was found to decrease the magnitude of:

$$\frac{d\alpha}{dt}$$

at $\psi = 0^\circ$ and 180° as can be deduced from the results presented in Fig 5. From Fig 5 it is seen that the best case for study is where $\mu = 0.22$. For this flight, the variation of C_N with azimuth is reproduced in Fig 10 where a similar plot is superimposed from the most appropriate oscillatory aerofoil test. The mean value and amplitude for the C_N variation is seen to be very closely matched, with a frequency that gives approximately the correct reduced value with an aerofoil model that has a chord that is 18% of the full scale value. As the comparison was to use existing oscillatory aerofoil data, it was not possible to obtain an exact match of reduced frequency. The selected Mach number for the comparison was 0.5, which was obtained in flight at azimuth angles of 8.6° and 171°. As it happened, the values of C_N at these two positions were exactly the same, and upper surface pressure distributions are shown in Fig 11. Here, pressure coefficient is plotted against $\sqrt{x/c}$ in order to spread out the leading-edge region. Also plotted in Fig 11 is the pressure distribution measured in the wind-tunnel in steady conditions, and there is remarkably little sign of unsteady effects in the flight results. It should be noted that there is also very little difference in C_m at the two azimuth positions.

In contrast, there are more marked unsteady effects found in the oscillatory aerofoil measurements as shown in Fig 12. On the left are shown the upper surface pressure distributions for the upstroke and downstroke when $C_N = 0.85$, at a reduced frequency that is only a little greater than for the flight results. Pressure distributions on the right are for a much higher frequency and clearly show how unsteady effects increase with frequency. Clearly, more comparisons between flight and oscillatory aerofoil tests are needed, but this first comparison suggests that unsteady Mach number effects tend to cancel the unsteady incidence effects over the fore and aft sectors of the rotor.

4 UNSTEADY EFFECTS ON THE ADVANCING BLADE

It is to be expected that there will be unsteady effects due to pitch rates on the advancing blade, and it is known that there are pronounced effects due to fluctuations in the blade Mach number, particularly when the flow over the blade is supercritical. However, demonstrations of the unsteady Mach number effects have been for non-lifting rotors[2], but two-dimensional prediction methods have been shown to be capable of reproducing these effects, and these could be used to determine whether or not unsteady Mach number effects and unsteady incidence effects tend to reinforce or cancel each other. This point is of course important when modelling unsteady effects in rotor loads prediction methods.

Before turning to the theoretical methods it is interesting to find out if there is any sign of unsteady effects in flight. Fig 13 shows the variation of C_N and C_m with azimuth, as measured on the modified Puma blade at a fairly high advance ratio. Also shown is the variation of blade Mach number at the measuring station. As M does not exceed 0.74 there will be no particularly well developed supercritical flow and unsteady Mach number effects are likely to be small (large effects are observed only when large changes in shock position occur). However, even though the variation of C_N is roughly symmetrical about the 90° azimuth position, the variation of C_m is not, having a definite nose-down change for $\psi > 90^\circ$. A change of this type would in fact be expected due to oscillatory pitch effects alone. The more interesting case where Mach number is higher would be found closer to the blade tip, but unfortunately there were no flight measurements in this region. We thus turn to theoretical studies to see if any important lessons are to be learnt.

Using the method described in Ref 3 the pressure distribution on a NACA 0012 aerofoil was calculated during the combined variations of Mach number and incidence shown below:

$$M = 0.558 + 0.217 \sin 2\Pi ft$$

$$\alpha = 3 - 3 \sin 2\Pi ft$$

where f is frequency and t is time.

The Mach number variation is that that would be found at 90% rotor radius when the tip Mach number due to rotation alone is 0.62 and the advance ratio 0.35, which is a typical cruise condition. The frequency and chord were chosen to give a reduced frequency of 0.076, based on half chord and the blade velocity at 0.9R due to rotation only. This is then equivalent to a rectangular blade of aspect ratio 7.3 which is about half the conventional value. Any unsteady effects will therefore be more pronounced than on a conventional blade. It should also be noted that viscous effects are not included in the calculation. The predicted variation of C_L and C_m with incidence or Mach number is shown in Fig 14, and unsteady effects are clearly evident. In order to assess the influence of oscillatory Mach number, Fig 14 also gives values of C_L and C_m that are predicted for each combination of M and α

when the free-stream Mach number is held steady at that particular value. For each calculation, the reduced frequency was set to the value appropriate to the value of Mach number in question. This latter prediction is equivalent to the way in which unsteady effects are usually introduced into rotor loads calculations, being based on oscillatory aerofoil characteristics in a steady free-stream. It is seen that when the oscillatory Mach number is neglected, then unsteady effects are magnified at the higher values of free-stream Mach number, where, as we see in Fig 15, the flow over the aerofoil is supercritical. Where the flow is sub-critical, there are no significant effects of the oscillatory Mach number.

The reason for the differences in pressure distribution seen in the bottom left hand corner of Fig 15 can be demonstrated qualitatively in Fig 16 where the three pressure distributions from the combined Mach number and incidence oscillation case are exactly the same as those on the left side of Fig 15. Also shown are pressure distributions at the same angles of incidences for the oscillatory incidence case with Mach number held constant at 0.75. At any point in either cycle, the pressure distribution must be influenced by its immediate history, and it is seen that the bottom distribution has been reached after a history of practically sub-critical flow in the oscillatory Mach number case, but of well developed supercritical flow for the steady Mach number case.

The particular case that was chosen for Fig 15 was not a particularly severe one as far as supercritical flow is concerned, and in many cases the tip of the advancing blade of a helicopter will penetrate much further into supercritical conditions, where unsteady effects should be much stronger. Fig 17 shows a further comparison of pressure distributions resulting from the same incidence variation and frequency as before but with a Mach number variation given by:

$$M = 0.638 + 0.212 \sin 2\Pi ft$$

The pressure distributions in Fig 17 are all for $\alpha = 1.5$ and compare the oscillatory Mach number case with the results of calculations at a fixed Mach number of 0.75, which is the value of M at $\alpha = 1.5$ in the oscillatory Mach number case. In the top part of the figure we see that if the variations of Mach number are neglected when α is decreasing then the shock wave is too strong and too far back on the aerofoil, giving a much larger value of C_L and a nose-down contribution to C_m. For incidence increasing, the bottom figure shows the reverse effect. These results emphasise the importance of unsteady effects in supercritical flow, but demonstrate that such effects are much smaller when Mach number is varying than would be deduced on the basis of pitch oscillations alone.

CONCLUSIONS

Various aspects of unsteady aerodynamic effects, as they occur on the helicopter rotor, have been examined with the possible influence of the oscillatory Mach number especially in mind. The results obtained so far lead us towards the following conclusions.

a. Two-dimensional oscillatory aerofoil tests give a close simulation of dynamic stall as it occurs on the retreating side of the rotor, in terms of the maximum value of C_N that can be achieved without stall and in the post-stall behaviour of lift and pitching-moment.

b. Unsteady effects over the fore and aft sectors of the rotor disc appear to be less than would be expected on the basis of oscillatory pitching effects alone. This may be due to unsteady Mach number influence.

c. On the advancing side of the disc there are strong unsteady effects due to unsteady Mach number when the flow is supercritical. However, the combined effects of oscillatory Mach number and incidence are much less than would be expected on the basis of pitch rates alone. Unsteady Mach number effects need to be included in the calculation of rotor loads.

REFERENCES

1	P G Wilby	The aerodynamic characteristics of some new RAE blade sections, and their potential influences on rotor performance. Vertica, Vol 4, pp121 to 133 (1980) Proceedings of Fifth European Rotorcraft and Powered Lift Aircraft Forum (1979)
2	F X Caradonna J J Philippe	The flow over a helicopter blade tip in the transonic regime. ONERA TP No 1976-115 (1976)
3	J Grant	A method for computing steady or time dependent two-dimensional supercritical flow about an aerofoil with application to a helicopter rotor. RAE TR 79084 (1979)

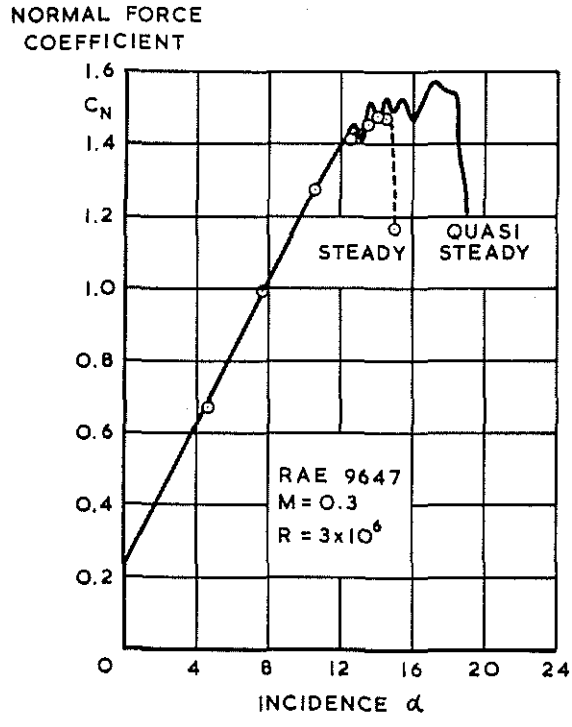

Fig 1 Variation of normal force coefficient with incidence as measured in two-dimensional wind-tunnel tests

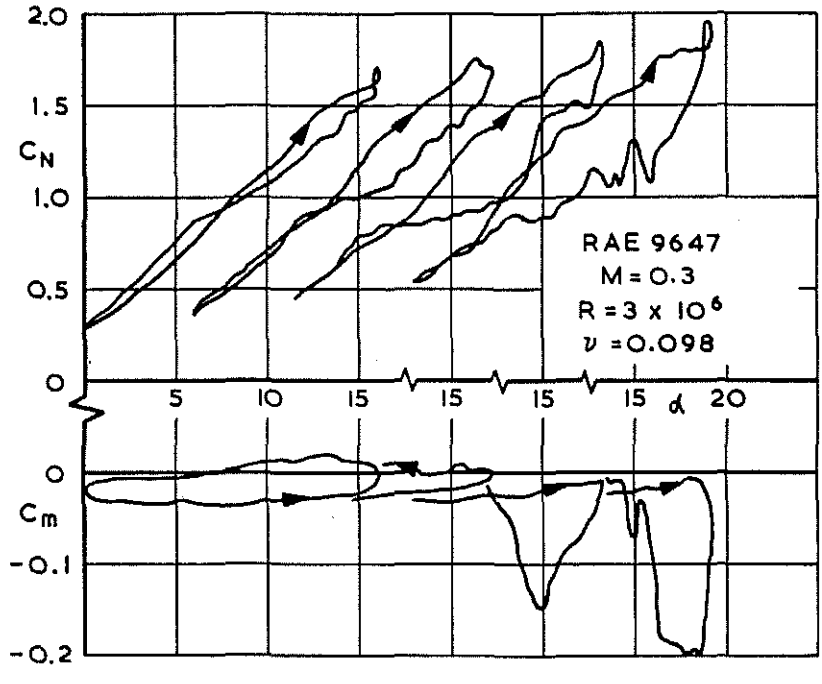

Fig 2 Variation of normal force and pitching-moment coefficients with incidence measured during pitch oscillations

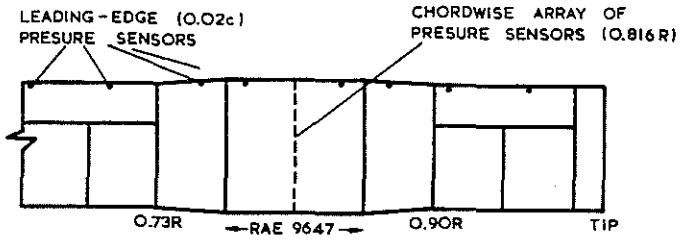

Fig 3 Modified blade and pressure sensor array for Puma flight experiment

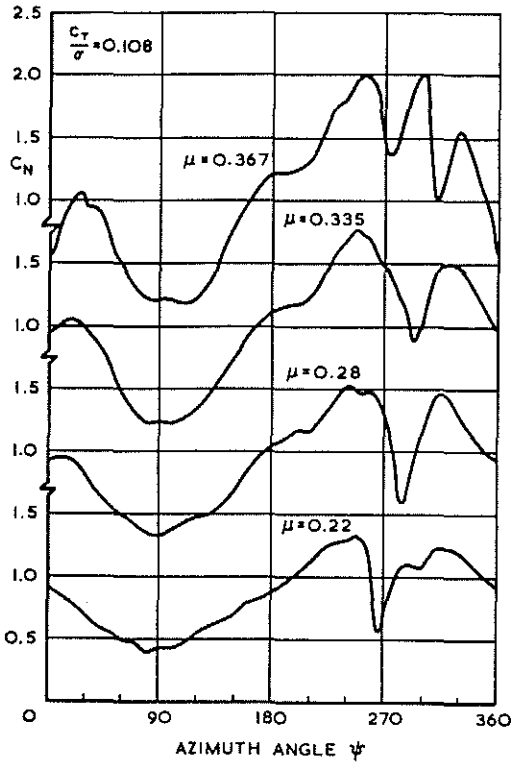

Fig 5 Variation of normal force coefficient with azimuth measured in flight for a range of advance ratio

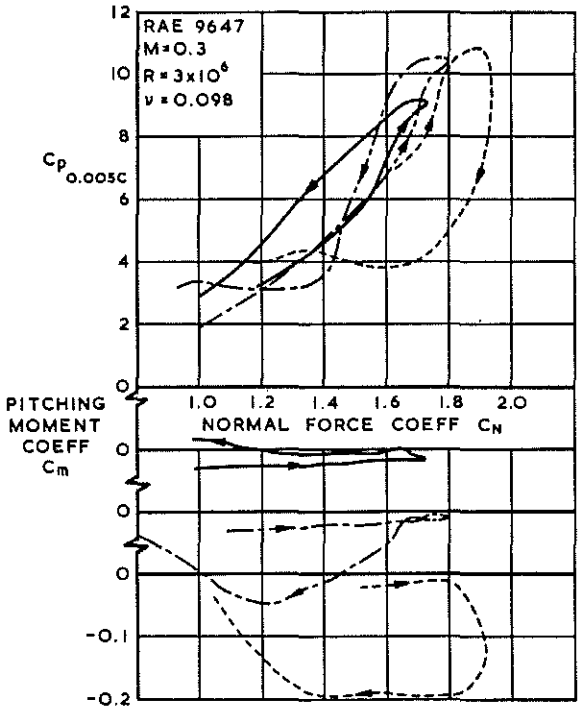

Fig 4 Variation of leading-edge pressure coefficient and pitching-moment coefficient with normal force coefficient measured in oscillatory pitch

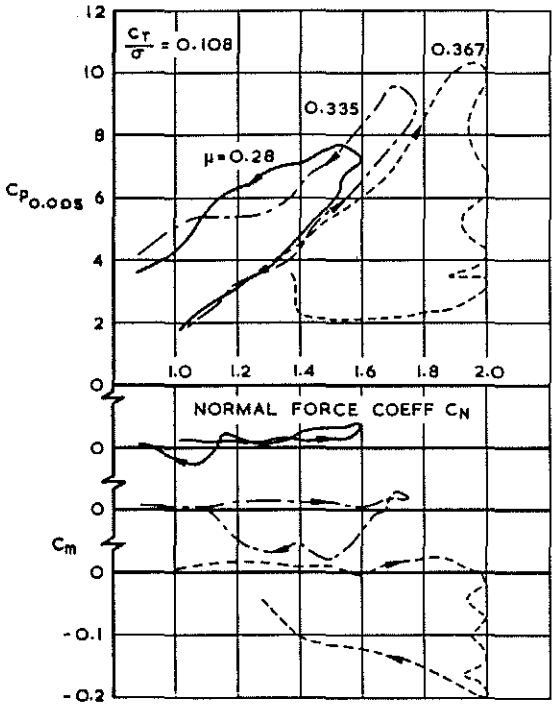

Fig 6 Variation of leading-edge pressure coefficient and pitching-moment coefficient with normal force coefficient measured in flight

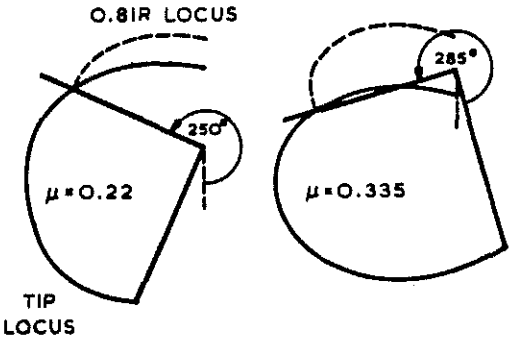

Fig 7 Intersection of measuring station (0.81R) with tip locus for preceding blade tip

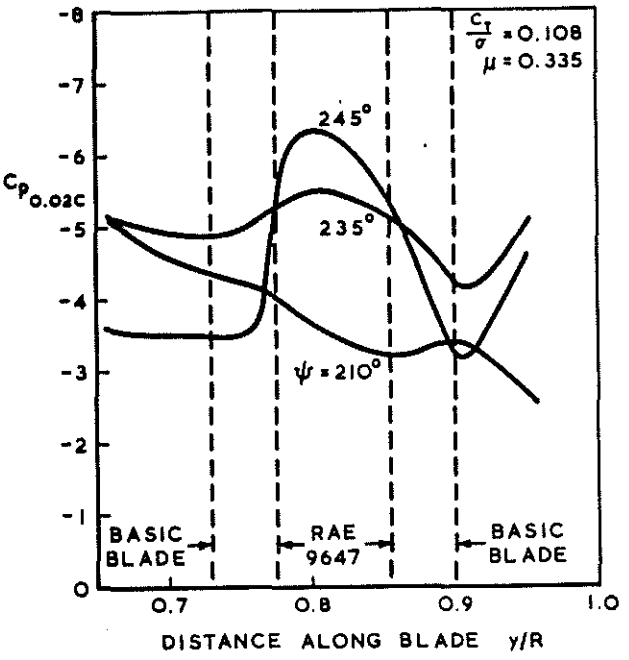

Fig 9 Spanwise distribution of leading-edge pressure coefficient at various azimuth positions

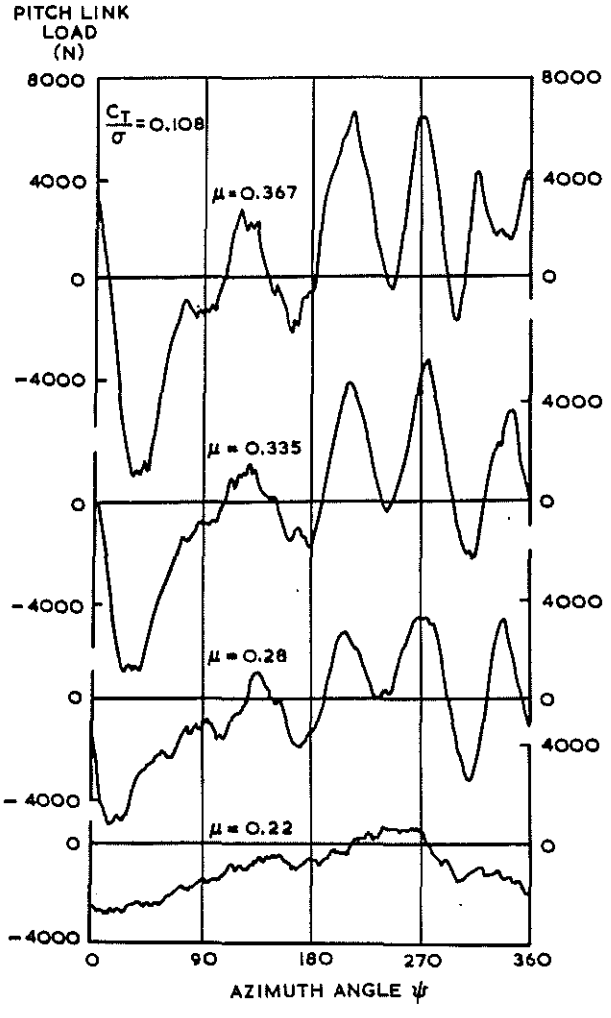

Fig 8 Pitch link load measured in flight for a range of advance ratio

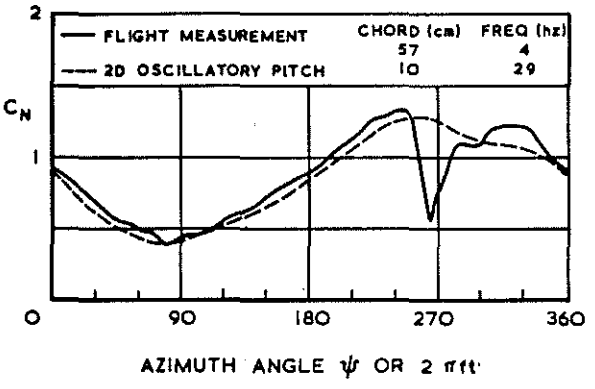

Fig 10 Variation of normal force coefficient through one cycle for comparative flight and oscillatory pitch tests

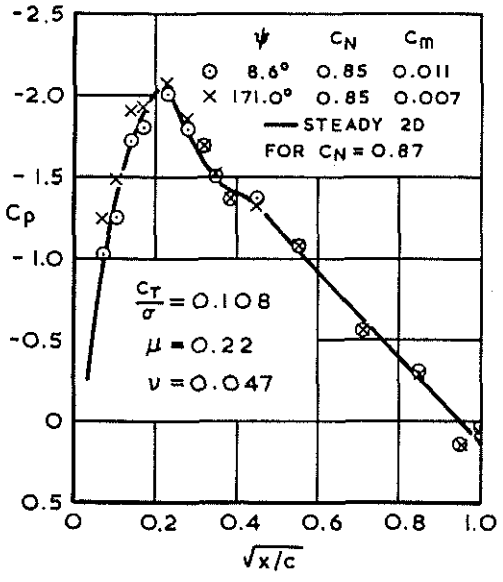

Fig 11 Upper surface pressure distributions measured in flight

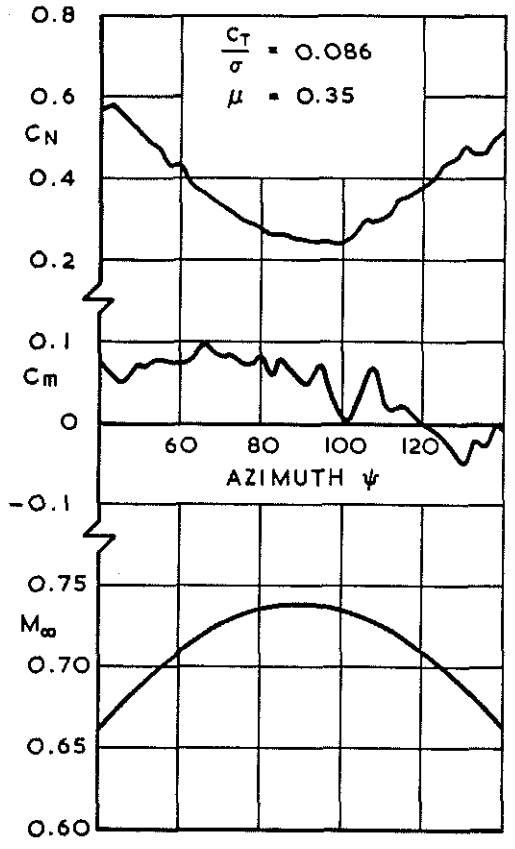

Fig 13 Variation of normal force and pitching-moment coefficient measured in flight on advancing blade

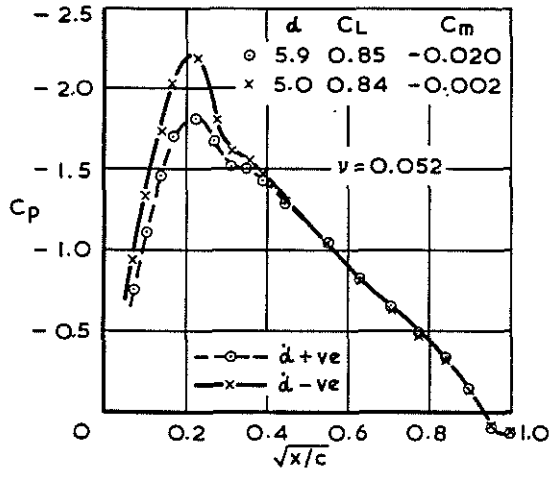

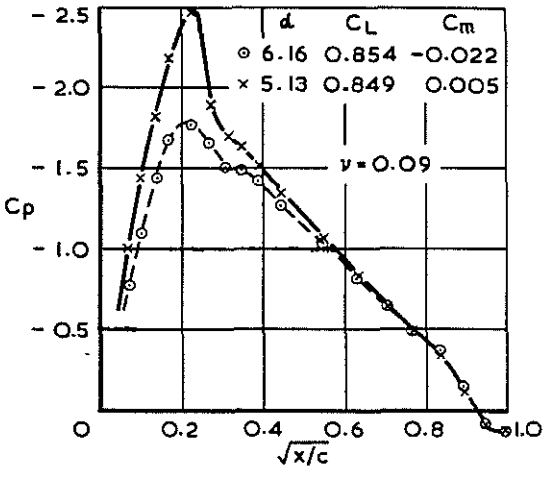

Fig 12 Upper surface pressure distributions measured in wind-tunnel oscillatory pitch tests at M = 0.51

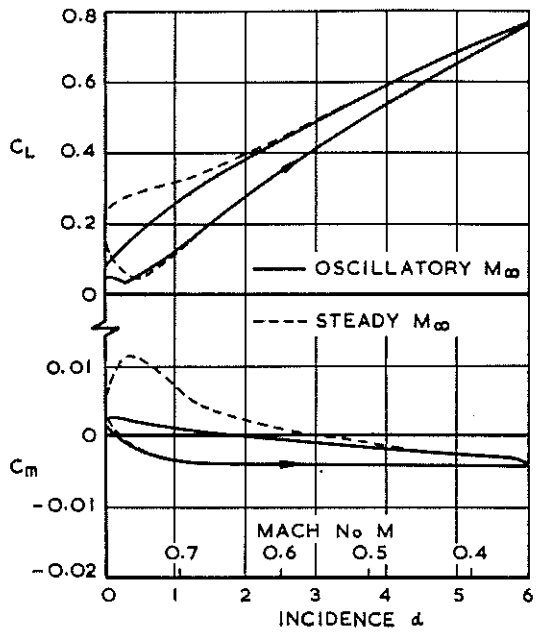

Fig 14 Theoretical variation of lift and pitching-moment coefficients for NACA 0012 under oscillatory pitch in inviscid flow, showing effect of oscillating free-stream Mach number

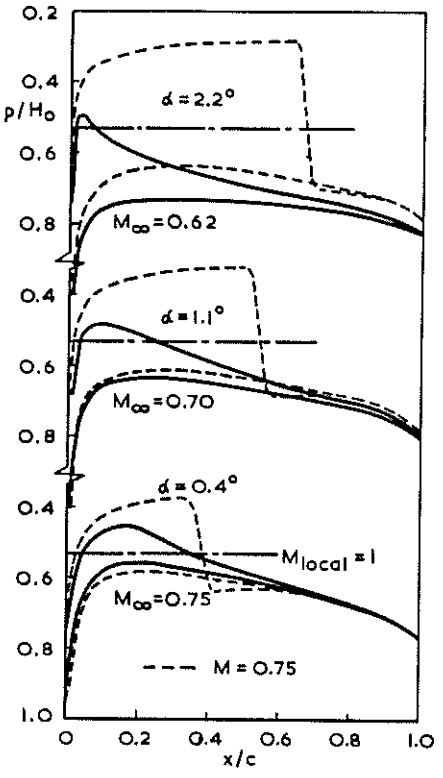

Fig 16 Theoretical pressure distributions for NACA 0012 under oscillatory pitch

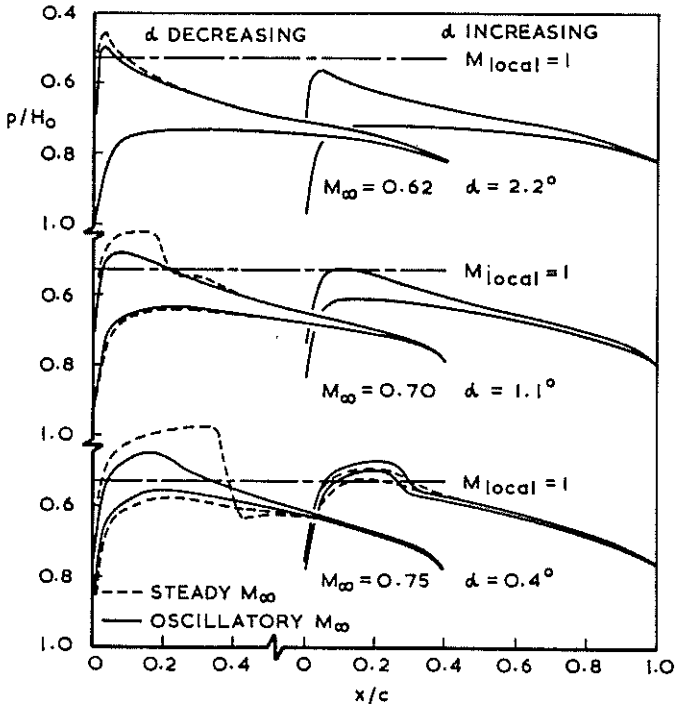

Fig 15 Theoretical pressure distributions for NACA 0012 under oscillatory pitch in inviscid flow, showing effect of oscillatory free stream Mach number

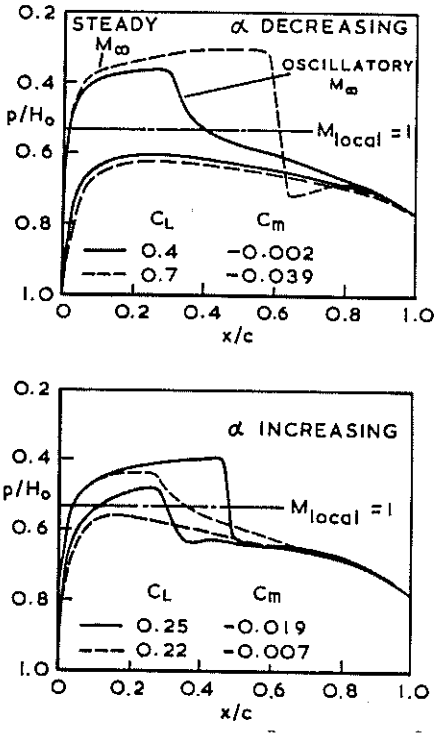

Fig 17 Theoretical pressure distributions for NACA 0012 under oscillatory pitch in inviscid flow; M = 0.75, $\alpha = 1.5°$